Novel mechanism of inhibition of human angiotensin-I-converting enzyme (ACE) by a highly specific phosphinic tripeptide

Mohd AKIF*, Sylva L. SCHWAGER†, Colin S. ANTHONY†, Bertrand CZARNY‡, Fabrice BEAU‡, Vincent DIVE‡, Edward D. STURROCK† and K. Ravi ACHARYA*[1]

*Department of Biology and Biochemistry, University of Bath, Claverton Down, Bath BA2 7AY, U.K., †Division of Medical Biochemistry and Institute of Infectious Disease and Molecular Medicine, University of Cape Town, Observatory 7935, South Africa, and ‡CEA, iBiTecS, Service d'Ingénierie Moléculaire des Protéines (SIMOPRO), Gif sur Yvette, F-91191, France

Human ACE (angiotensin-I-converting enzyme) has long been regarded as an excellent target for the treatment of hypertension and related cardiovascular diseases. Highly potent inhibitors have been developed and are extensively used in the clinic. To develop inhibitors with higher therapeutic efficacy and reduced side effects, recent efforts have been directed towards the discovery of compounds able to simultaneously block more than one zinc metallopeptidase (apart from ACE) involved in blood pressure regulation in humans, such as neprilysin and ECE-1 (endothelin-converting enzyme-1). In the present paper, we show the first structures of testis ACE [C-ACE, which is identical with the C-domain of somatic ACE and the dominant domain responsible for blood pressure regulation, at 1.97Å (1 Å = 0.1 nm)] and the N-domain of somatic ACE (N-ACE, at 2.15Å) in complex with a highly potent and selective dual ACE/ECE-1 inhibitor. The structural determinants revealed unique features of the binding of two molecules of the dual inhibitor in the active site of C-ACE. In both structures, the first molecule is positioned in the obligatory binding site and has a bulky bicyclic P_1' residue with the unusual R configuration which, surprisingly, is accommodated by the large S_2' pocket. In the C-ACE complex, the isoxazole phenyl group of the second molecule makes strong pi–pi stacking interactions with the amino benzoyl group of the first molecule locking them in a 'hand-shake' conformation. These features, for the first time, highlight the unusual architecture and flexibility of the active site of C-ACE, which could be further utilized for structure-based design of new C-ACE or vasopeptidase inhibitors.

Key words: angiotensin-1-converting enzyme (ACE), cardiovascular disease, crystal structure, inhibitor design, metalloprotease.
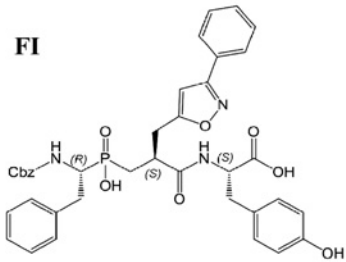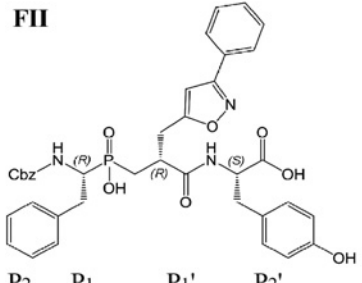
INTRODUCTION

Membrane-bound zinc metallopeptidases such as ACE (angiotensin-I-converting enzyme, EC 3.4.15.1), NEP (neutral endopeptidase, also known as neprilysin, EC 3.4.24.11) and ECE-1 (endothelin-converting enzyme-1, EC 3.4.24.71) exert vasoconstrictive and vasodilatory activities [via Ang-II (angiotensin-II), and ET-1 (endothelin-1), and natriuretic peptides and BK (bradykinin) respectively] and are well-established targets for the treatment of cardiovascular disease [1–6]. Despite the success of ACE inhibitor therapy in the treatment of hypertensive patients, it has been established that chronic use of these inhibitors causes undesirable side effects, such as persistent dry cough, loss of taste and angiooedema, which are most likely due to elevated levels of BK [7,8]. Moreover, ACE inhibition can induce an increase in chymase activity in cardiac interstitial fluid, providing an alternative pathway for the formation of Ang-II [9]. Hence, blood pressure control remains suboptimal in a significant proportion of patients on this therapy, as well as those on other antihypertensive drug treatments [10]. This provides a compelling case for the development of new improved strategies for the treatment of patients with high blood pressure, a major risk factor for cardiovascular complications. To address this concern, potent vasopeptidase inhibitors able to target ACE and NEP were first developed [11,12], followed by dual NEP/ECE-1 inhibitors and ultimately triple inhibitors

blocking ACE/NEP/ECE-1 simultaneously [13]. Even though the dual ACE/NEP inhibitor omapatrilat was more clinically efficacious than a single ACE inhibitor, the higher incidence of angiooedema observed in patients treated with omapatrilat halted the development of omapatrilat and raised concerns about the risk/benefit ratio of dual ACE/NEP inhibitors for therapeutic applications [14]. Although the incidence of angiooedema associated with triple ACE/NEP/ECE-1 inhibitor treatment is yet to be evaluated, it has been suggested that NEP inhibition (in the context of either dual or triple inhibitor treatment) might be responsible for the increase in adverse effects [13]. Indeed it has been established that inhibition of NEP results in increased levels of BK and ET-1. These data initiated the development of novel inhibitors that interact with the C-domain of ACE (C-ACE) and ECE-1 [15] (Figure 1). The discovery of the first potent and selective dual C-ACE/ECE-1 inhibitors revealed that the configuration of the P_1' residue was a key factor in the control of inhibitor selectivity (Figure 1). Instead of the classical S configuration in the P_1' position of the inhibitor (corresponding to an L amino acid, as observed in all ACE inhibitors reported to date) (compound FI in Figure 1), we discovered that an R configuration in compounds (compound FII in Figure 1) containing long and bulky P_1' side chains was well accommodated by ACE, as well as by ECE-1, but much less so by NEP (for details see [15]). Furthermore, in a spontaneous hypertensive rat model, an intravenous administration of a C-ACE/ECE-1 dual inhibitor (FII)

Figure 1   Chemical structures of ACE/ECE-1 dual inhibitors FI and FII and their potency

Compound FI adopts the *S* configuration and compound FII adopts the *R* configuration.

(10 mg/kg of body weight) lowered the mean arterial blood pressure by 24 ± 2 mmHg (1 mmHg = 0.133 kPa) as compared with controls [15].

In humans there are two ACE isoforms: somatic ACE, which comprises two homologous enzymatic domains (N- and C- with $\sim 60\%$ amino acid sequence identity) [16] and testis ACE, which is a single domain protein identical with the C-domain of somatic ACE [17]. Although both cleave angiotensin-I, it has been shown that C-ACE is sufficient to maintain the regulation of blood pressure *in vivo* [18] and hence viewed as the dominant site of Ang-II generation. On the other hand the N-domain (N-ACE) contributes to the regulation of haemopoietic stem cell differentiation and proliferation through its hydrolysis of the anti-fibrotic haemoregulatory peptide AcSDKP (AZ-acetyl-seryl-aspartyl-lysyl-proline, a biological substrate of ACE) [19,20]. In addition, these domains have their own distinctive physiochemical properties, such as thermostability [21], resistance to proteolysis [22], chloride-ion dependence [23,24] and substrate preference [19,25,26]. Subtle differences in the crystal structures of the apo and bound forms of the two domains have been exploited for the development of domain-selective ACE inhibitors [27–33].

In order to gain structural insight into the dual ACE/ECE-1 inhibitor (FII) binding to ACE we have determined the crystal structure of FII in complex with C-ACE and N-ACE at high resolution. In the present paper we describe the novel and unexpected binding features of a highly specific and unusual dual inhibitor FII.

EXPERIMENTAL

Synthesis of the phosphinic tripeptide (FII) [(2S)-2-({3-[hydroxyl(2-phenyl-(1R)-1-{[(benzyloxy)carbonyl]-amino}eth-yl)phosphinyl]-2-[(3-phenylisoxazol-5-yl)methyl]-1-oxo-propyl}amino)-3-(4-hydroxy-phenyl) propanoic acid] was performed as described by Jullien et al. [15]. Potency of inhibitors towards C-ACE and N-ACE, as well as potency towards NEP and ECE-1, were determined as described by Jullien et al. [15,34]. K_i values

were determined at $25\,^{\circ}\mathrm{C}$ in 50 mM Hepes (pH 6.8), 200 mM NaCl, 10 μM $ZnCl_2$ and 0.02 % Brij-35.

Protein purification and crystallization of ACE/ECE-1 dual inhibitor (FII) complex

C-ACE

A variant of human testis ACE (tACEΔ36-g13, underglycosylated protein) was purified to homogeneity from CHO (Chinese-hamster ovary) cells, as described previously [35]. The crystals of the C-ACE complex with the dual inhibitor were grown at $16\,^{\circ}\mathrm{C}$ by the hanging-drop vapour diffusion method. C-ACE protein (11.5 mg/ml in 50 mM Hepes, pH 7.5) was pre-incubated with FII (1 mM) on ice for 5 h before crystallization. The pre-incubated sample (2 μl) was mixed with the reservoir solution consisting of 13.5 % PEG [poly(ethylene glycol)] 4000, 50 mM sodium acetate (pH 4.7) and 10 μM $ZnSO_4$, and suspended above the well. Diffraction quality co-crystals appeared after approximately 1 week.

N-ACE

The minimally glycosylated construct of the N-domain of somatic ACE, N-ACE389, was generated by site-directed mutagenesis, as described previously [33]. The recombinant protein was expressed in CHO cells and purified to homogeneity by lisinopril affinity chromatography. The crystals of N-ACE in complex with FII were grown at $16\,^{\circ}\mathrm{C}$ by the hanging-drop method. An initial hit was obtained in the presence of 0.06 M divalent cations, 0.1 M Tris/Bicine (pH 8.5) and 30 % PEG 550MME/PEG 20000, and was refined using the Hampton Research silver bullets additive screen. Briefly, the N-ACE protein (4 mg/ml) was pre-incubated with FII (at a molar ratio of 1:5) on ice before crystallization, 2 μl of pre-incubated sample was mixed with 1 μl of reservoir solution and 1 μl of G3 of silver bullet condition No 3 and suspended above the well. Diffraction quality crystals appeared after approximately 1 week.
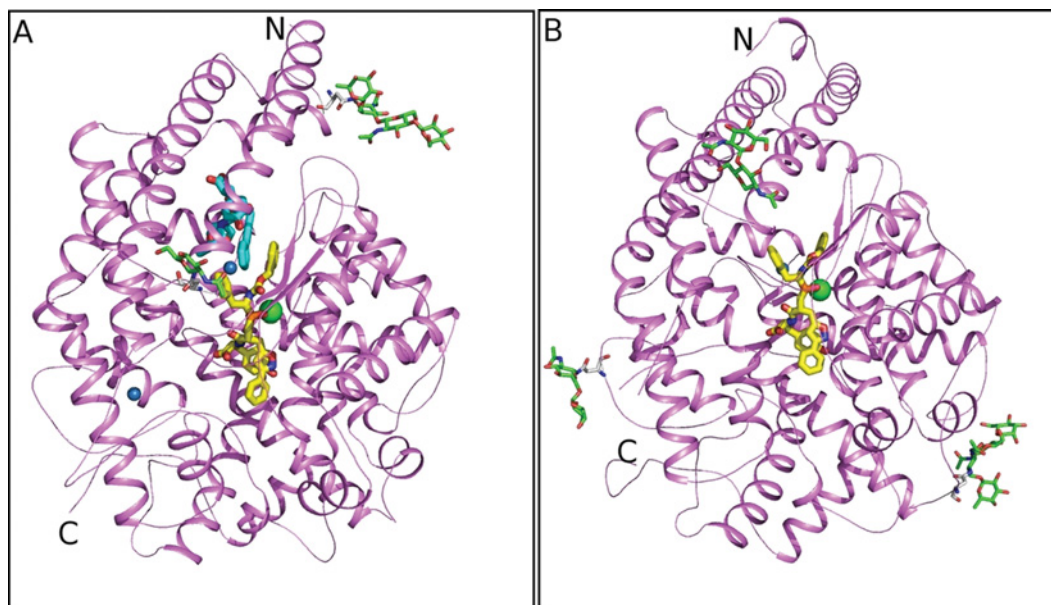
Figure 2   Overall topology of C-ACE and N-ACE molecules

(**A**) A cartoon representation of the C-ACE structure with bound dual-inhibitor molecules at sites A and B (FII-A and FII-B) and the observed N-glycosylated sugars (green sticks) at the N-glycosylation sites (Asn[72] and Asn[109]). The bound inhibitor molecules at the two sites, FII-A and F II-B, are shown in stick representation, coloured in yellow and cyan respectively. The active-site Zn^{2+} ion and the location of the two Cl^{−} ions are shown in green and skyblue spheres respectively. (**B**) A cartoon representation of N-ACE in complex with the dual inhibitor. The bound dual inhibitor (FII) and the N-glycosylated sugars are shown as yellow and green sticks respectively. The Zn^{2+} ion and the bound Cl^{−} ion are also shown and coloured as in C-ACE.

Data collection and structure determination

Two datasets were collected on stations IO3 and IO4 at Diamond Light Source. No cryoprotectant was used to keep the crystal at constant temperature (100K) under the liquid nitrogen jet during data collection. Raw data images were indexed and scaled with the HKL2000 software package [36]. Data reduction was carried out using the CCP4 program TRUNCATE [37]. The structures were solved by molecular replacement using PHASER [38] with the aid of the native C-ACE (PDB code 1O86) [27] and N-ACE (PDB code 2C6F) [29] structures as search models. The resultant structures were refined for stereochemically restrained positional and temperature factors using REFMAC5 [39]. In total 5 % of reflections were separated as the R_{free} set and used for cross validation [40]. Manual adjustments of the models were carried out using COOT [41]. Water molecules were added at positions where $F_o−F_c$ electron density peaks exceeded 3σ and potential hydrogen bonds could be made. On the basis of clear electron density interpretation, two FII molecules in the C-ACE complex structure and one FII molecule in the N-ACE structure were added and further refinement was carried out. The co-ordinate and parameter files for FII were generated using the PRODRG server [42]. Structure validation was conducted with the aid of programs PROCHECK [43] and MOLPROBITY [44]. There were no residues in the disallowed region of the Ramachandran plot. Figures 2 and 3 were drawn with PyMOL (http://www.pymol.org). Hydrogen bonds were verified with the program HBPLUS [45]. Details of crystallographic data are given in Table 1.

RESULTS AND DISCUSSION

Overall structures

For the crystal structure determination an underglycosylated form of C-ACE was used that only had two of the potential seven N-linked glycans. Although it is possible that introducing mutations to disrupt glycosylation sites may affect the structure of a protein, previous work has shown that enzymatically deglycosylated C-ACE, as well as various glycosylation mutants of N- and C-ACE, have comparable enzymatic activities to the WT (wild-type) forms [33,35,46]. These findings imply that the crystal structures of minimally glycosylated N- and C-ACE are likely to be highly informative of the WT structures. Furthermore, aligning the X-ray structures of minimally glycosylated N- and C-ACE to the structures of their WT forms revealed RMSDs (root mean square deviations) for all atoms of 0.70 Å (1 Å = 0.1 nm) and 0.51 Å for the N- and C-ACE comparisons respectively. Thus the minimally glycosylated structures of the N- and C-domains are essentially identical with their glycosylated counterparts, and mutation of the glycan sequons does not seem to affect the structure or function of the enzyme.

The C-ACE structure in complex with FII (one molecule per asymmetric unit) was refined to 1.97 Å resolution. No noticeable conformational change was observed in the structure upon inhibitor binding (RMSDs of 0.38 and 0.51 Å for Cα atoms and all atoms respectively). This is consistent with the previously determined structures of C-ACE inhibitor complexes [27,28,30–32]. The overall protein structure (Figure 2A) contains a Zn^{2+} ion, two Cl^{−} ions, two molecules of FII (for details see below), one Hepes molecule (from the crystallization medium), partially visible N-linked glycans at two potential glycosylation sites (Asn[72] and Asn[109]) and 563 water molecules (Table 1).

The N-ACE structure in complex with FII (two molecules per asymmetric unit) was refined to 2.15Å resolution. As in the case of previously determined N-ACE complexes [29,33], no noticeable conformational change was observed in the structure upon inhibitor binding (RMSDs of 0.56 and 0.70 Å for Cα atoms and all atoms respectively). The overall protein structure (Figure 2B) contains a Zn^{2+} ion, one Cl^{−} ion per molecule, one
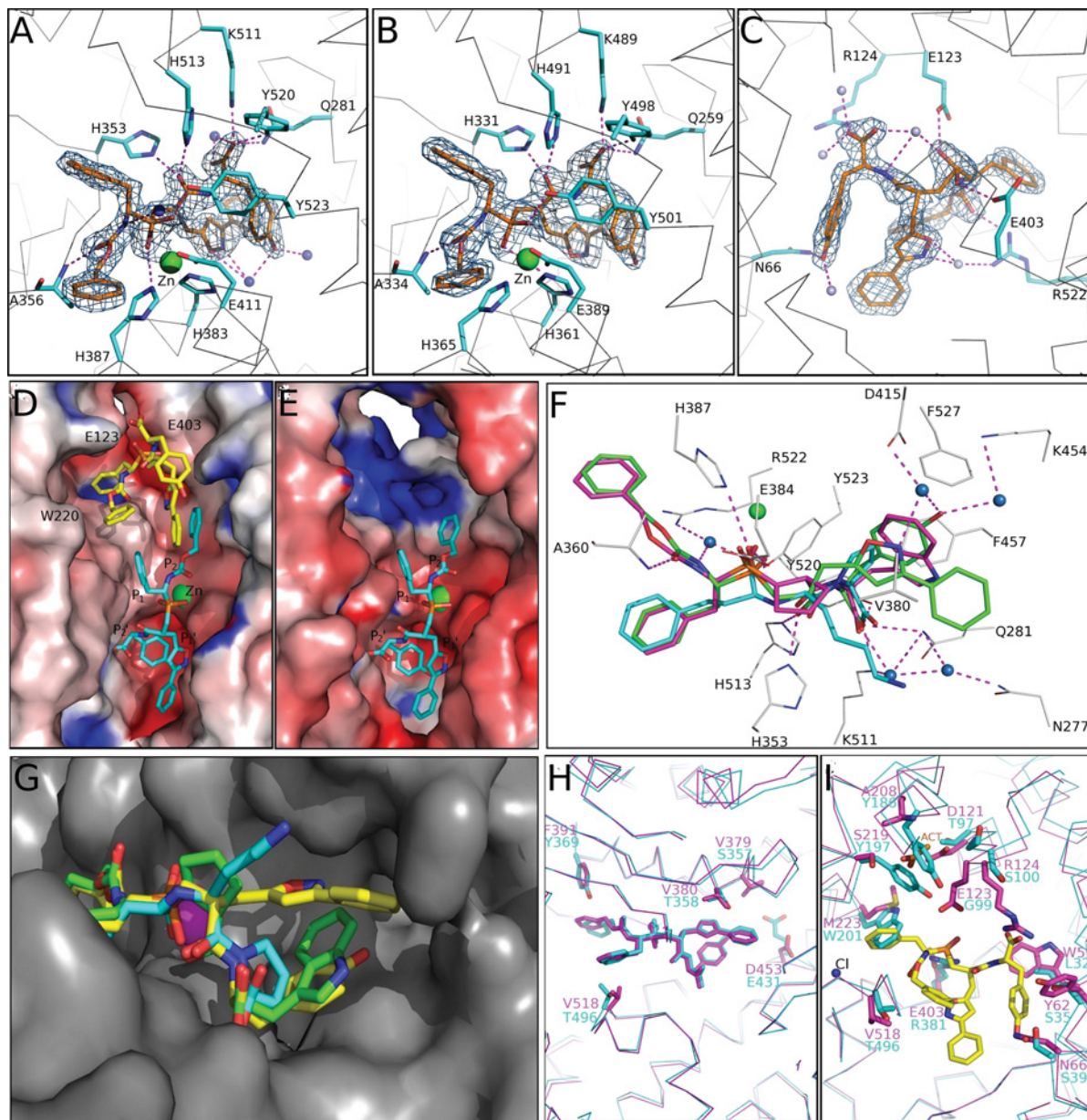
Figure 3   Details of FII binding in C-ACE and N-ACE active sites

(**A**–**C**) Close-up views of the active site showing bound inhibitors. (**A**) Interaction for C-ACE with the dual inhibitor at the primary site FII-A. (**B**) Interaction for N-ACE with the dual inhibitor at the primary site FII-A. (**C**) Interaction of C-ACE with the dual inhibitor at the secondary binding site FII-B. The interacting residues in the active site are labelled. The electron density map shown is the F_o-F_c map contoured at 3σ level. The Zn^{2+} ion and water molecules are in green and sky-blue spheres, and the inhibitor molecules are shown in stick representation. (**D** and **E**) Surface diagram with inhibitors showing their potential arrangement in C-ACE and N-ACE. (**D**) C-ACE with two FII molecules (sites A and B) bound at the active-site cavity. The isoxazole phenyl group of the second molecule makes a strong pi–pi stacking interaction with the amino benzoyl group of the first molecule locking them in a 'hand-shake' conformation. (**E**) N-ACE with a single dual inhibitor in the active site at (site FII-A). (**F**) The orientation of dual inhibitor (FII) in comparison with other known inhibitors. Comparison of the orientation of FII binding (the present study) against previously reported lisinopril [27] and RXPA380 [30] in the active site of the C-ACE. FII (green sticks), lisinopril (PDB code 1O86; cyan sticks) and RXPA380 (PDB code 2CO2; magenta sticks) bound in the active site of co-crystal structures of C-ACE are superimposed. The Zn^{2+} ion and water molecules are shown as green and sky-blue spheres. Active-site residues of C-ACE interacting with FII are labelled and their hydrogen-bond interactions are shown as magenta dotted lines. (**G**). Comparison of the orientation of the dual inhibitor (*S* configuration; FI, yellow sticks) compared with lisinopril (cyan sticks) [27] and RXPA380 (green sticks) [30] from their respective complexes with C-ACE. (**H** and **I**) Comparison of dual-inhibitor-binding sites in C-ACE with N-ACE. (**H**) Superimposition of dual-inhibitor binding FII-A in C-ACE (magenta) with dual-inhibitor binding in N-ACE (cyan). The dual inhibitors are shown in stick representation, and differences in residues near the dual-inhibitor-binding site in both structures are labelled (magenta, C-ACE; cyan, N-ACE). (**I**) Superimposition of dual-inhibitor binding FII-B in C-ACE with N-ACE (purple). Residues from C-ACE and N-ACE are labelled in magenta and cyan respectively. The dual inhibitor FII-B is shown in yellow stick representation.

molecule of FII (for details see below) each monomer, five PEG molecules of different lengths (from the crystallization medium), partially visible N-linked glycans at three potential glycosylation sites (Asn[45], Asn[416] and Asn[480]) and a total of 663 water molecules (Table 1).

Novel inhibitor-binding mode

C-ACE–FII complex

Two bound inhibitor molecules were identified unambiguously in the C-ACE active site in close proximity to one another,

Table 1 Crystallographic statistics for the ACE/ECE-1 dual inhibitor FII complex

Values in parentheses are for last resolution shell.

Statistic	C-ACE	N-ACE
Resolution (Å)	1.97	2.15
Space group	$P2_12_12_1$	$P1$
Number of molecules/ASU	1	2
Cell dimensions		
a,b,c	58.7, 86.1, 134.8Å	89.1, 64.4, 75.8Å
α,β,γ	90, 90, 90°	78.8, 76.4, 82.9°
Total number of observations	526714	718177
Number of unique reflections	49449	84896
Completeness (%)	97.8 (93.4)	97.0 (95.0)
$I/\sigma(I)$	15.6 (3.3)	14.1 (2.4)
R_{symm}*	7.4 (31.4)	7.3 (48.1)
R_{cryst}†/R_{free}‡	19.8/23.2	21.9/25.5
Deviation from ideality		
Bond lengths (Å)	0.007	0.008
Bond angles (°)	1.204	1.16
B-factor analysis (Å²)		
Protein atoms (chain A/B)	20.8	33.7/39.2
Solvent atoms	28.2	33.1
Inhibitor atoms	17.4	32.3/34.1
Zn^{2+} ion (chain A/B)	14.5	25.1/23.6
Glycosylated sugars	47.4	58.6/71.5
Hepes atoms	64	
Cl^- ions (2) (chain A/B)	14.6	23.8/31.6
PEG atoms (chain A/B)		57.0/55.8

*$R_{symm} = \Sigma_h \Sigma_i [|I_i(h) - <I(h)>| / \Sigma_h \Sigma_i I_i(h)]$, where I_i is the ith measurement and $<I(h)>$ is the weighted mean of all the measurements of $I(h)$.

†$R_{cryst} = \Sigma_h |F_o - F_c| / \Sigma_h F_o$, where F_o and F_c are observed and calculated structure factor amplitudes of reflection h respectively.

‡R_{free} is equal to R_{cryst} for a randomly selected 5 % subset of reflections.

by inspection of the Fourier difference electron density map (Figures 3A and 3C). One molecule (hereafter called FII-A, the primary site) occupies the expected S_1, S_2, S_1' and S_2' subsites of the C-ACE active site, whereas the unexpected second molecule (hereafter called FII-B, the secondary site) forms intermolecular aromatic (pi–pi) interactions with FII-A through a 'hand-shake' conformation and extends towards the non-primed region of the active site involving some 46 contacts (Figure 3D).

FII-A binding

The phosphoryl zinc-binding group of FII-A interacts with the catalytic Zn^{2+} ion through its two oxygen atoms (distances of 2.04 Å and 2.74 Å respectively). However, the accommodation of the unusual P_1' side chain with the R configuration of FII-A in the active site of C-ACE has resulted in a significantly different positioning of the inhibitor. This can be seen by comparing the superimposition of the binding modes of lisinopril (a well-known clinically used ACE inhibitor with a K_i values of 44 and 2.4 nM for N-ACE and C-ACE of human somatic ACE respectively [23,27]), RXPA380 [a C-ACE-specific phosphinic inhibitor with a K_i value of 3 nM (2500 nM for N-ACE)] [30,47] and FII-A (Figure 3F).

Despite different chemical structures and the zinc-binding groups, the backbone of lisinopril and RXPA380 inhibitors, as well as the orientation of their respective side chains, superimpose well [30] (Figure 3F). In contrast, comparing the binding mode of FII-A to either that of lisinopril or RXPA380 reveals a different picture. There is a marked difference in the positioning of FII-A

in the C-ACE active site and, more specifically, the positioning of its phosphoryl zinc-binding group and the orientation of the inhibitor molecule at the P_1, P_1' and P_2' positions. In the P_1' position, the nitrogen atom of the isoxazole ring is held by a water-mediated interaction with Asp[415]. The oxygen atom of the isoxazole ring appears to make a direct interaction with the active-site residue His[383]. Surprisingly, the bulky side chain of FII at the P_1' position points in an unusual orientation and extends towards the S_2' pocket. This particular orientation is probably stabilized by hydrophobic interactions provided by Val[380] and the P_1' aromatic ring of the inhibitor molecule (Figure 3F), but it is also rendered possible by the unique topology of the S_1' and S_2' subsites of ACE, which form a single and very large cavity, sufficiently wide enough to accept the bulky P_1' side chain in the S or R configuration (Figure 3G). In the S configuration, the P_1' side chain would probably assume an orientation similar to that observed for the lysine residue in lisinopril. In addition to these points, several polar and van der Waals interactions observed between FII and ACE, as compared with more 'classical ACE inhibitors' (see below), are probable reasons why inhibitors FI and FII exhibit similar potency towards ACE.

The C-terminal tyrosine side chain at the P_2' position of the inhibitor is held by hydrophobic interactions mediated through aromatic residues Phe[527] and Phe[457], an orientation slightly different to that adopted by the tryptophan side chain of RXPA380 (Figure 3F). Furthermore, the hydroxy group of the tyrosine moiety of the inhibitor is anchored via water-mediated hydrogen bonds with Asp[415], His[383] and Lys[454]. The phenyl side chain at the P_1 position is held by hydrophobic interactions provided by the side chains of Phe[512] and Val[518]. Finally, the phenyl group at the P_2 position of the dual inhibitor makes aromatic contact with Phe[391], as observed for RXPA380 [30]. Despite this unusual binding mode, FII-A is involved in strong interactions with the protein atoms: 16 hydrogen bonds, which include seven water-mediated hydrogen bonds, as calculated by HBPLUS (Figure 3A and Table 2); and several atoms of FII-A are in close proximity to ten protein side chains (Ser[355], Glu[376], Val[379], Val[380], Phe[391], His[410], Phe[457], Phe[512], Val[518] and Phe[527]), most of them making extensive van der Waals contacts. This network of interactions provides an excellent structural basis for the sub-nanomolar affinity of this dual inhibitor towards ACE.

FII-B binding

For the first time, an inhibitor molecule is observed at a secondary binding site (FII-B) in the ACE structure. The inhibitor is held by nine water-mediated hydrogen bonds and two direct interactions with Asn[66] and Arg[522], as calculated by HBPLUS (Table 2). In addition, Glu[123], Glu[403] and Arg[124] also mediate direct interactions with the inhibitor (Figure 3C). The isoxazole phenyl of FII-B makes strong aromatic (pi–pi) stacking interactions with the amino benzoyl group of inhibitor FII-A at the primary site (Figure 3D). The P_1 phenyl group of the dual inhibitor participates in an aromatic interaction with Trp[220] of the protein molecule. The isoxazole phenyl group of FII-B makes an aromatic interaction with Trp[357] and the tyrosine group at the P_2' position of FII-B appears to make a hydrophobic interaction with Tyr[62]. The phosphinic oxygen atoms appear to make direct interactions with Glu[123] and Glu[403], and a weak interaction with Lys[118]. In the native C-ACE structure, and in all previously studied C-ACE inhibitor-bound complexes [27,28,30,31], this binding site of FII-B is occupied by a string of bound water molecules.

Table 2   Comparison of hydrogen-bond interactions with the dual inhibitor FII in C-ACE and N-ACE complexes

Domain	Site	Inhibitor atoms	Interacting protein atoms	Distance (Å)
C-ACE	Primary (FII-A)	O	Q281NE2	3.02
		OAC	H353NE2	2.61
		OAB	A356N	2.87
		OAG	H383NE2	3.15
		OAG	H387NE2	3.06
		O	K511NZ	2.69
		OAC	H513NE2	2.83
		O	Y520OH	2.59
		OAD	Y523OH	2.59
		NBI	Wat	3.10
		OXT	Wat	2.69
		O	Wat	3.45
		OH	Wat	2.80
		OH	Wat	2.76
		OBK	Wat	3.36
		NBG	Wat	2.81
	Secondary (FII-B)	OH	N66ND2	3.13
		OAB	R522NH2	3.05
		OAD	Wat	2.46
		OAC	Wat	2.61
		N	Wat	3.28
		OXT	Wat	2.81
		OXT	Wat	2.86
		O	Wat	2.54
		OH	Wat	2.72
		OBK	Wat	3.22
		NBG	Wat	2.66
N-ACE	Primary	O	Q259NE2	3.00
		OAC	H331NE2	2.64
		OAB	A334N	2.76
		NBG	T358OG1	3.45
		OAG	H365NE2	2.90
		O	K489NZ	2.62
		OAC	H491NE2	2.98
		O	Y498OH	2.58
		OAD	Y501OH	2.53
		*	*	*
		NBI	Wat	2.99
		OXT	Wat	2.67
		OH	Wat	2.44

*Additional contacts identified for the second molecule in the asymmetric unit at the primary-binding site.

N-ACE–FII complex

One bound inhibitor molecule per monomer of FII was found in the primary site (FII-A, occupying all four substrate binding sites: S_2, S_1, S_1' and S_2') and was identified unambiguously in the active site of N-ACE (Figures 3B and 3E). No secondary FII-binding site was observed. As in the case of the C-ACE–FII complex (described above), the binding pocket retains the full complement of conserved hydrogen-bond interactions in the N-ACE active site (Figure 3B and Table 2). The phenyl group at the P_2 position of FII is held by hydrophobic interactions mediated through His[388] and Tyr[369]. The second phenyl group at the P_1 position of FII appears to make aromatic interactions with Phe[490]. The oxygen of the bulky isoxazole ring at the P_1' position makes a direct interaction with the ND1 atom of His[361], whereas the nitrogen atom of the isoxazole ring appears to participate in a weak hydrogen-bond interaction with the OG1 atom of Thr[358]. The hydroxy group of the tyrosine moiety at the P_2' position of FII is held by direct interactions with the OD2 atom of Asp[393], and by weak interactions with the NZ atom of Lys[432]. In addition, Ser[333], His[388], Phe[435], Phe[490], Thr[496] and Phe[505] also make hydrophobic interactions with the inhibitor.

However, a structure-based alignment of residues from the two complexes revealed some significant differences in residues at the periphery of this primary site (Figure 3H).

A comparison of the N-ACE active site with the FII-B-binding site of C-ACE clearly showed the presence of several key residues occluding the binding of FII. Specifically, Leu[32], Ser[35], Val[36], Trp[203] and Arg[381] in the N-ACE active site are replaced by Trp[59], Tyr[62], Ala[63], Met[223] and Glu[403] in the C-ACE respectively (Figure 3I). These observations provide a structural basis for the lower specificity of FII for N-ACE as compared with C-ACE.

Conclusion

The S_1' pocket of ACE can accommodate a variety of P_1' residues including alanine, histidine, phenylalanine and lysine with its more extended conformation. However, our structural data did not reveal any direct interactions between the bulky bicyclic P_1' group of FII-A and the S_1' pocket but, unexpectedly, this side chain was oriented more towards the S_2' pocket, rationalizing the accommodation of a bulky P_1' group in the R configuration by the active site. It should be noted that an S configuration of the P_1' residue was reported to be an absolute requirement in all clinical ACE inhibitors [15]. As shown in the present study, the accommodation of an R configuration not only concerns the orientation of the phenyl-isoxazole side chain, but also implies a striking shift in positioning of FII-A in the C-ACE and N-ACE active site, compared with the binding modes of other known ACE inhibitors. Despite this particular binding mode, FII-A has been shown to be engaged in multiple polar and non-polar interactions, an observation that expands the current 'dogma' regarding the chemical space defined by the ACE active sites.

In addition, the unexpected observation of the binding of the dual inhibitor at the secondary site of C-ACE, FII-B, (involving displacement of conserved water molecules), provides further leads to be explored with regard to subtle modifications of the chemical space at the active site. It also demonstrates the active-site plasticity in accommodating potent inhibitors. Thus the present study for the first time has provided a wealth of fundamental knowledge about ACE/ECE-1 dual-inhibitor (FII) specificity which will no doubt prove useful in understanding the selectivity profiles of different vasoactive hormones.

REFERENCES

1 Petrillo, E. W. J. and Ondetti, M. A. (1982) Angiotensin-converting enzyme inhibitors: medicinal chemistry and biological actions. Med. Res. Rev. **2**, 1–41

2 Roques, B. P., Noble, F., Daugé, V., Fournié-Zaluski, M. C. and Beaumont, A. (1993) Neutral endopeptidase 2411: structure, inhibition, and experimental and clinical pharmacology. Pharmacol. Rev. **45**, 87–146

3 Jeng, A. Y. (2003) Utility of endothelin-converting enzyme inhibitors for the treatment of cardiovascular diseases. Curr. Opin. Investig. Drugs **4**, 1076–1081

4 Acharya, K. R., Sturrock, E. D., Riordan, J. F. and Ehlers, M. R. W. (2003) ACE revisited: a new target for structure-based drug design. Nat. Rev. Drug Discovery **2**, 891–902

5 Cerdeira, A. S., Brás-Silva, C. and Leite-Moreira, A. F. (2008) Endothelin-converting enzyme inhibitors: their application in cardiovascular diseases. Rev. Port. Cardiol. **27**, 385–408

6 Dive, V., Chang, C., Yiotakis, A. and Sturrock, E. D. (2009) Inhibition of zinc metallopeptidases in cardiovascular disease: from unity to trinity, or duality? Curr. Pharm. Des. **15**, 3606–3621

7 Antonios, T. F. and MacGregor, G. A. (1995) Angiotensin converting enzyme inhibitors in hypertension: potential problems. J. Hypertens. Suppl. **13**, S11–S16

8 Israili, Z. H. and Hall, W. D. (1992) Cough and angioneurotic edema associated with angiotensin-converting enzyme inhibitor therapy. A review of the literature and pathophysiology. Ann. Intern. Med. **117**, 234–242

9 Wei, C. C., Hase, N., Inoue, Y., Bradley, E. W., Yahiro, E., Li, M., Naqvi, N., Powell, P. C., Shi, K., Takahashi, Y. et al. (2010) Mast cell chymase limits the cardiac efficacy of Ang I-converting enzyme inhibitor therapy in rodents. J. Clin. Invest. **120**, 1229–1239

10 Elijovich, F. and Laffer, C. (2009) A role for single-pill triple therapy in hypertension. Ther. Adv. Cardiovasc. Dis. **3**, 231–240

11 Gros, C., Noël, N., Souque, A., Schwartz, J. C., Danvy, D., Plaquevent, J. C., Duhamel, L., Duhamel, P., Lecomte, J. M. and Bralet, J. (1991) Mixed inhibitors of angiotensin-converting enzyme and enkephalinase: rational design, properties, and potential cardiovascular applications of glycopril and alatriopril. Proc. Natl. Acad. Sci. U.S.A. **88**, 4210–4214

12 Worthley, M. I., Corti, R. and Worthley, S. G. (2004) Vasopeptidase inhibitors: will they have a role in clinical practice? Br. J. Clin. Pharmacol. **57**, 27–36

13 Daull, P., Jeng, A. Y. and Battistini, B. (2007) Towards triple vasopeptidase inhibitors for the treatment of cardiovascular diseases. J. Cardiovasc. Pharmacol. **50**, 247–256

14 Campbell, D. J. (2003) Vasopeptidase inhibition: a double-edged sword? Hypertension **41**, 383–389

15 Jullien, N., Makritis, A., Georgiadis, D., Beau, F., Yiotakis, A. and Dive, V. (2010) Phosphinic tripeptides as dual angiotensin-converting enzyme C-domain and endothelin-converting enzyme-1 inhibitors. J. Med. Chem. **53**, 208–220

16 Soubrier, F., Alhenc-Gelas, F., Hubert, C., Allegrini, J., John, M., Tregear, G. and Corvol, P. (1988) Two putative active centers in human angiotensin I-converting enzyme revealed by molecular cloning. Proc. Natl. Acad. Sci. U.S.A. **85**, 9386–9390

17 Ehlers, M. R. and Riordan, J. F. (1989) Angiotensin-converting enzyme: new concepts concerning its biological role. Biochemistry **28**, 5311–5318

18 Fuchs, S., Xiao, H. D., Hubert, C., Michaud, A., Campbell, D. J., Adams, J. W., Capecchi, M. R., Corvol, P. and Bernstein, K. E. (2008) Angiotensin-converting enzyme C-terminal catalytic domain is the main site of angiotensin I cleavage *in vivo*. Hypertension **51**, 267–274

19 Rousseau, A., Michaud, A, Chauvet, M. T., Lenfant, M. and Corvol, P. (1995) The hemoregulatory peptide N-acetyl-Ser-Asp-Lys-Pro is a natural and specific substrate of the N-terminal active site of human angiotensin-converting enzyme. J. Biol. Chem. **270**, 3656–3661

20 Li, P., Xiao, H. D., Xu, J., Ong, F. S., Kwon, M., Roman, J., Gal, A., Bernstein, K. E. and Fuchs, S. (2010) Angiotensin-converting enzyme N-terminal inactivation alleviates bleomycin-induced lung injury. Am. J. Pathol. **177**, 1113–1121

21 Voronov, S., Zueva, N., Orlov, V., Arutyunyan, A. and Kost, O. (2002) Temperature-induced selective death of the C-domain within angiotensin-converting enzyme molecule. FEBS Lett. **522**, 77–82

22 Sturrock, E. D., Danilov, S. M. and Riordan, J. F. (1997) Limited proteolysis of human kidney angiotensin-converting enzyme and generation of catalytically active N- and C-terminal domains. Biochem. Biophys. Res. Commun. **236**, 16–19

23 Wei, L., Clauser, E., Alhenc-Gelas, F. and Corvol, P. (1992) The two homologous domains of human angiotensin I-converting enzyme interact differently with competitive inhibitors. J. Biol. Chem. **267**, 13398–13405

24 Jaspard, E., Wei, L. and Alhenc-Gelas, F. (1993) Differences in the properties and enzymatic specificities of the two active sites of angiotensin I-converting enzyme (kininase II). Studies with bradykinin and other natural peptides. J. Biol. Chem. **268**, 9496–9503

25 Deddish, P. A., Jackman, H. L., Skidgel, R. A. and Erdös, E. G. (1997) Differences in the hydrolysis of enkephalin congeners by the two domains of angiotensin converting enzyme. Biochem. Pharmacol. **53**, 1459–1463

26 Deddish, P. A., Marcic, B., Jackman, H. L., Wang, H. Z., Skidgel, R. A. and Erdös, E. G. (1998) N-domain-specific substrate and C-domain inhibitors of angiotensin-converting enzyme: angiotensin-(1–7) and keto-ACE. Hypertension **31**, 912–917

27 Natesh, R., Schwager, S. L. U., Sturrock, E. D. and Acharya, K. R. (2003) Crystal structure of the human angiotensin-converting enzyme-lisinopril complex. Nature **421**, 551–554

28 Natesh, R., Schwager, S. L. U., Evans, H. R., Sturrock, E. D. and Acharya, K. R. (2004) Structural details on the binding of antihypertensive drugs captopril and enalaprilat to human testicular angiotensin I-converting enzyme. Biochemistry **43**, 8718–8724

29 Corradi, H. R., Schwager, S. L. U., Nchinda, A. T., Sturrock, E. D. and Acharya, K. R. (2006) Crystal structure of the N domain of human somatic angiotensin I-converting enzyme provides a structural basis for domain-specific inhibitor design. J. Mol. Biol. **357**, 964–974

30 Corradi, H. R., Chitapi, I., Sewell, B. T., Georgiadis, D., Dive, V., Sturrock, E. D. and Acharya, K. R. (2007) The structure of testis angiotensin-converting enzyme in complex with the C domain-specific inhibitor RXPA380. Biochemistry **46**, 5473–5478

31 Watermeyer, J. M., Kröger, W. L., O'Neill, H. G., Sewell, B. T. and Sturrock, E. D. (2008) Probing the basis of domain-dependent inhibition using novel ketone inhibitors of angiotensin-converting enzyme. Biochemistry **47**, 5942–5950

32 Watermeyer, J. M., Kröger, W. L., O'Neill, H. G., Sewell, B. T. and Sturrock, E. D. (2010) Characterization of domain-selective inhibitor binding in angiotensin-converting enzyme using a novel derivative of lisinopril. Biochem. J. **428**, 67–74

33 Anthony, C. S., Corradi, H. R., Schwager, S. L. U., Redelinghuys, P., Georgiadis, D., Dive, V., Acharya, K. R. and Sturrock, E. D. (2010) The N domain of human angiotensin-I converting enzyme: the role of N-glycosylation and the crystal structure in complex with an N domain specific phosphinic inhibitor RXP407. J. Biol. Chem. **285**, 35685–35693

34 Jullien, N. D., Cuniasse, P., Georgiadis, D., Yiotakis, A. and Dive, V. (2006) Combined use of selective inhibitors and fluorogenic substrates to study the specificity of somatic wild-type angiotensin-converting enzyme. FEBS J. **273**, 1772–1781

35 Gordon, K., Redelinghuys, P., Schwager, S. L. U., Ehlers, M. R. W., Papageorgiou, A. C., Natesh, R., Acharya, K. R. and Sturrock, E. D. (2003) Deglycosylation, processing and crystallization of human testis angiotensin-converting enzyme. Biochem. J. **371**, 437–442

36 Otwinoswski, Z. and Minor, W. (1997) Processing of X-ray diffraction data collected in oscillation mode. Methods Enzymol. **276**, 307–326

37 Collaborative Computational Project, Number 4 (1994) The CCP4 suite: programs for protein crystallography. Acta Crystallogr. Sect. D Biol. Crystallogr. **50**, 760–763

38 McCoy, A. J., Grosse-Kunstleve, R. W. P., Adams, P. D., Winn, M. D., Storoni, L. C. and Read, R. J. (2007) PHASER crystallographic software. J. Appl. Crystallogr. **40**, 658–674

39 Murshudov, G. N., Vagin, A. A. and Dodson, E. J. (1997) Refinement of macromolecular structures by the maximum-likelihood method. Acta Crystallogr. Sect. D Biol. Crystallogr. **D53**, 240–255

40 Brünger, A. T. (1992) Free R value: a novel statistical quantity for assessing the accuracy of crystal structures. Nature **355**, 472–475

41 Emsley, P. and Cowtan, K. (2004) COOT: model-building tools for molecular graphics. Acta Crystallogr. Sect. D Biol. Crystallogr. **D60**, 2126–2132

42 Schüttelkopf, A. W. and van Aalten, D. M. F. (2004) PRODRG: a tool for high-throughput crystallography of protein-ligand complexes. Acta Crystallogr. Sect. D Biol. Crystallogr. **D60**, 1355–1363

43 Laskowski, R. A., Moss, D. S. and Thornton, J. M. (1993) Main-chain bond lengths and bond angles in protein structures. J. Mol. Biol. **231**, 1049–1067

44 Davis, I. W., Leaver-Fay, A., Chen, V. B., Block, J. N., Kapral, G. J., Wang, X., Murray, L. W., Arendall, III, W. B., Snoeyink, J., Richardson, J. S. and Richardson, D. C. (2007) MOLPROBITY: all-atom contacts and structure validation for proteins and nucleic acids. Nucleic Acids Res. **35**, W375–W383

45 McDonald, I. K. and Thornton, J. M. (1994) Satisfying hydrogen bonding potential in proteins. J. Mol. Biol. **238**, 777–793

46 Yu, X. C., Sturrock, E. D., Wu, Z., Biemann, K., Ehlers, M. R. and Riordan, J. F. (1997) Identification of N-linked glycosylation sites in human testis angiotensin-converting enzyme and expression of an active deglycosylated form. J. Biol. Chem. **272**, 3511–3519

47 Georgiadis, D., Cuniasse, P., Cotton, J., Yiotakis, A. and Dive, V (2004) Structural determinants of RXPA380, a potent and highly selective inhibitor of the angiotensin-converting enzyme C-domain. Biochemistry **43**, 8048–8054